Revista Brasileira de Ciência do Solo

Division - Soil Use and Management | Commission - Soil and Water Management and Conservation

Sediment Morphology, Distribution, and Recent Transport Dynamics in a Reforested Fragment

Renata Cristina Bovi[(1)], Laura Fernanda Simões da Silva[(2)], Mariana Delgado Oliveira Zenero[(1)], Camila Carolina de Carvalho[(3)] and Miguel Cooper[(4)*]

[(1)] Universidade de São Paulo, Escola Superior de Agricultura "Luiz de Queiroz", Departamento de Ciência do Solo, Programa de Pós-graduação em Solos e Nutrição de Plantas, Piracicaba, São Paulo, Brasil.
[(2)] Universidade Federal de São Carlos, Centro de Ciências Agrárias, Programa de Pós-Graduação em Agroecologia e Desenvolvimento Rural, São Carlos, São Paulo, Brasil.
[(3)] Universidade de São Paulo, Escola Superior de Agricultura "Luiz de Queiroz", Curso de Agronomia, Piracicaba, São Paulo, Brasil.
[(4)] Universidade de São Paulo, Escola Superior de Agricultura "Luiz de Queiroz", Departamento de Ciência do Solo, Piracicaba, São Paulo, Brasil.

Abstract: Erosion generates large amounts of sediment, which may be deposited at the site of origin, on the slope of a hill, or along waterways. The transportability of each type of sediment by runoff and its potential for subsequent deposition largely depends on its morphological features and particle size distribution. The aim of this study is to describe and characterize the morphology and micromorphology of sediments deposited in a reforested area and to understand the dynamics of the transport process. In order to understand the sedimentation processes, the following analyses were performed: particle size distribution, with and without the use of a dispersant solution; statistical analysis of the sand fraction using Folk and Ward parameters; sediment and soil micromorphology; and two-dimensional distribution and geometry of soil horizons and sediments. The sedimentation occurred in a localized and discontinuous manner and in the lowest parts of the landscape. The sediments were generated by low intensity erosive events producing well-sorted sediments and the clay in these deposits was transported mainly in the form of silt-sized clay aggregates. Microscopic analysis of the sediments was important for clarifying the genesis and transport dynamics of the sedimentary deposits.

Keywords: soil erosion, sedimentation, particle size, silting.

***Corresponding author:**
E-mail: mcooper@usp.br

Received: October 23, 2016
Approved: March 20, 2017

How to cite: Bovi RC, Silva LFS, Zenero MDO, Carvalho CC, Cooper M. Sediment morphology, distribution, and recent transport dynamics in a reforested fragment. Rev Bras Cienc Solo. 2017;41:e0160454.
https://doi.org/10.1590/18069657rbcs20160454

INTRODUCTION

Soil erosion is a process consisting of three phases: particle detachment from the soil mass, particle transport by erosive agents, and particle deposition (Sharma, 1996; Morgan, 2005). Water erosion is a significant environmental degradation process, the results of which include soil loss and reduced crop yield and water quality and quantity. The on-site and off-site impacts of accelerated erosion increase environmental degradation on a global scale (Ouyang et al., 2013; Borrelli et al., 2014; Pope and Odhiambo, 2014; Świtoniak, 2014; Wang et al., 2014) and have important economic and social implications (Telles et al., 2013).

Sediments are responsible for a decrease in water quality, through silting of rivers and drainage dikes, reduction in the lifespan of reservoirs, etc. (Young et al., 1987; Pimentel et al., 1995; Morgan, 2005). In view of these and other consequences, studies on sediment properties, such as particle size, mineralogy, texture, and grain orientation, are important since these characteristics are related to the physical and chemical factors of the depositional environment (van Lier and Vidal-Torrado, 1992).

Particle size distribution of sediments is determined by the properties of the source material (soil, rock, etc.), landscape, and rainfall amount and intensity. An analysis of this distribution elucidates the transport mechanism of these particles and their subsequent deposition in the lower compartments of the landscape (Harmon et al., 1989). Soil texture and degree of aggregation can affect the size of the aggregates that might remain stable during an erosion event. Thus, soils that exhibit high cohesion generate sediments partially consisting of primary particle aggregates, whereas low cohesion soils tend to produce sediments in the form of primary particles detached by the breakdown of the aggregates during the erosion process (Meyer et al., 1980).

Consequently, characterization of the particle size distribution of sediments must be carried out in a way that can measure either the particles dispersed by erosion or the particles transported in the form of aggregates (Momoli et al., 2007). Particle size distribution is also determined using water as a dispersant, as this represents an efficient simulation of the particle dispersion caused by rain or runoff (Meyer et al.,1980; Martínez-Mena et al., 1999; Martínez-Mena et al., 2002).

The energy of the water flow influences the resulting deposition pattern. Sediment deposition may be irregular, uneven, and poorly sorted where the intensity of erosion is high - turbulent flow, but where the intensity of erosion is low - non-turbulent flow - deposition patterns are regular and sediments are well-sorted (Suguio, 1973; Momoli et al., 2007). In order to understand the nature and intensity of the transport processes of detached soil material, statistical analyses of the sand fraction are carried out to quantify the average diameter, degree of sorting, kurtosis, and symmetry of the particle size distribution (Folk and Ward, 1957).

Numerous studies have been undertaken in order to understand and quantify the erosion process (Lima and Silva, 2007; Sveistrup et al., 2008; Nunes and Cassol, 2011; Santos and Sparovek, 2011). In contrast, few studies characterize the sediment generated by erosion in terms of its macro and micromorphology. These additional parameters are necessary for inferring the type of depositional environment and form of deposition.

Thus, the scientific question of this study is: what are the characteristics of the surface water flow that affect the morphology and distribution of the sediments found in the study area? To answer this question, the hypothesis is that sediments are derived from local erosion processes, and their deposition patterns depend on both low and high energy water flows. The aim of this study is to describe and characterize the morphology of soils and sediments deposited in a reforested area, and to understand the associated dynamics of sediment transport and deposition.

MATERIALS AND METHODS

The study area belongs to the Tupi Experimental Station, Piracicaba, SP, Brazil, a production/conservation unit of the Forestry Institute that belongs to the Environmental Agency of the State of São Paulo and is located between longitudes 47° 32' 30" W and 47° 31' 47" W and latitudes 22° 43' 21" S and 22° 44' 24" S (Figure 1). The local climate is humid subtropical, Cwa, according to the Köppen classification system. The average annual temperature is 22.4 °C and average annual rainfall is 1,275 mm, with a rainy season between October and March (data obtained from the Meteorological Station of the University of São Paulo in Piracicaba, SP, Brazil).

The land use and management of the Tupi Experimental Station was initially agriculture after deforestation in 1949; reforestation with Guarantã (*Esenbeckia leiocarpa*) and pine began in 1960. The parent materials of the study area are Paleozoic sedimentary rocks belonging to the Tubarão Group, represented predominantly by sandstones and sandy diamictites of the Itararé Group (sandy membrane) (Vidal-Torrado and Lepsch, 1999).

This study was conducted in a plot reforested in 1960 with *Pinus* spp and Guarantã (*Esenbeckia leiocarpa*). This plot, with an area of approximately 10,000 m², is located on the footslope and includes part of the drainage channel of the watershed. In this channel, a gully formed, which became the base level of the area and currently controls the water flow. To identify the presence of sediment deposits in this area, exploratory auger holes were drilled in a 5 × 5 m grid to a depth of 1.5 m.

These deposits were discovered from *in situ* observation of morphological differences between the layers, using color as a basic feature of identification. Based on this exploratory analysis, two pits were dug to a depth of 1.60 m, and named T1 and T2. Furthermore, two profiles on the walls of the gully were selected, which were named P1 and P2.

The soil profiles and pits were subsequently described in accordance with Santos et al. (2013b) and classified as Hapludults (Soil Survey Staff, 2014), corresponding to *Argissolo Vermelho Amarelo Distrófico típico* according to the Brazilian System of Soil Classification (Santos et al., 2013a). After description of the pits and profiles, the geometry of the soil horizons and sediment layers were defined along four toposequence segments, designated TP1, TP2, TP3, and TP4, using successive auger holes, based on the methodology proposed by Boulet et al. (1982). The inclination of the slope was identified using a clinometer, and the distances between auger holes were measured using a measuring tape.

For each soil horizon and sediment layer described in the pits and profiles, disturbed samples were collected for particle size and organic matter (OM) content analysis.

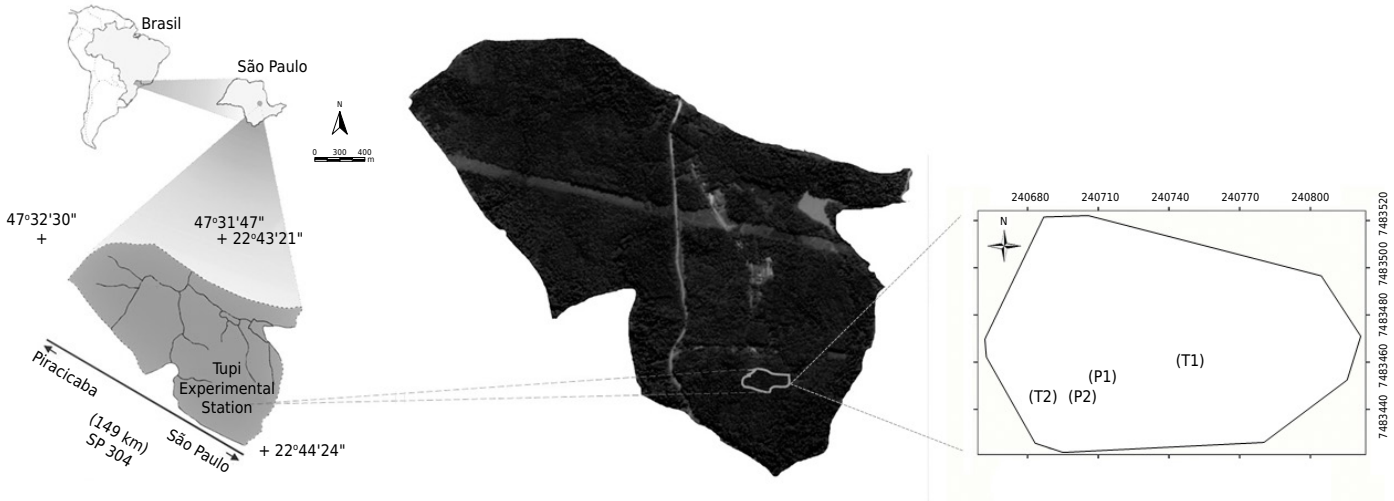

Figure 1. Location of the Tupi Experimental Station, and-highlighted, the area selected for this study.

Organic matter content was determined in accordance with Walkley-Black's method (Claessen, 1997). Particle size distribution was analyzed using the hydrometer method (Grossman and Reinsch, 2002), and the samples were divided into two groups: the first was dispersed with sodium hexametaphosphate solution ($Na_{16}P_{14}O_{43}$) and sodium hydroxide (NaOH) for total dispersion of the soil particles, and the second was dispersed only in water, following the method proposed by Gee and Or (2002).

The sand fraction resulting from particle size distribution analysis with dispersant solution was dried in an oven for 48 h and separated by sieves into five fractions: very coarse sand (> 1000 µm), coarse sand (from 500 to 1000 µm), medium sand (between 250 and 500 µm), fine sand (between 106 and 250 µm), and very fine sand (<106 µm). The result of this fractionation was statistically analyzed according to the parameters established by Folk and Ward (1957) with the assistance of the R package "rysgran" (Gilbert et al., 2012) to characterize the distribution of sand particles in the soil and sediment and understand the deposition dynamics.

Undisturbed samples with dimensions of 12 × 7 × 5 cm were collected from each soil horizon and sediment layer to carry out micromorphological analysis. The samples in the shape of blocks were impregnated following the method proposed by Murphy et al. (1977), Murphy (1986), and Castro et al. (2003). The impregnated and hardened blocks were cut into 0.5 cm thick slices for preparation of thin sections with dimensions of 4.5 × 7 cm for posterior micromorphological description (Castro et al., 2003).

The thin sections were analyzed in a polarizing Zeiss optical microscope and a Zeiss binocular stereoscope under both plane-polarized light (PPL) and cross-polarized light (XPL). The descriptions followed the criteria and terminology proposed by Bullock et al. (1985) and Stoops (2003), and identification of the relative distribution followed the classification of Stoops and Jongerius (1975).

RESULTS AND DISCUSSION

Morphological characterization of the soil horizons and sediment layers

The morphological properties and organic matter content of the soil horizons and sediment layers in the pits and profiles studied are shown in table 1. The morphological description showed differences between the soil horizons and sediment layers.

In T1, the following sequence of soil horizons and sediment layers was found: A, sediment, Ab, Eb, and Btb (Figure 2a). The color of the A horizon was 10YR 3/2 and the structure was weak, fine, and granular. The color of the sediment, which was 0.21 m thick, was 10YR 4/3 and had a simple grain structure differing in color and structure compared to both the under- and overlying horizons. The color of the Ab horizon was 10YR 4/2, with subangular blocks that were weak and medium sized, and the Ab horizon had the morphological feature of darker color (10YR 4/2) than the other horizons due to its higher OM content (10.5 g kg^{-1}). All horizons and sediment layers had a sandy texture, except for the Btb horizon, which had a sandy loam texture.

The T2 had the following sequence of soil horizons and sediment layers: A, sediment 1, sediment 2, Ab, Eb, and Btb (Figure 2b). The A horizon had a granular structure and weak, fine, subangular blocks, differing from the sediments, which had simple grain structure. Two sediment layers were identified, one, between 0.10 and 0.31 m, which featured the color 10YR 5/3 and another, between 0.31 and 0.41m, featuring the color 10YR 5/4. These layers differed from the overlying A horizon and the underlying Ab horizon both in terms of color (5YR 4/1 for both horizons) and structure. The Ab horizon had a medium subangular blocky structure with a small increase in OM content (7.6 g kg^{-1}) compared to the sediments deposited above. In this pit, only the Btb horizon showed a sandy loam texture; all other horizons were classified as having a sandy texture.

Table 1. Morphological properties and organic matter content (OM) in the soil horizons and sediment layers, described in the pits and profiles

Horizon	Layer	Color (humid) Munsell	Structure[(1)]	Texture	OM
	m				g kg^{-1}
		Pit 1 – T			
A	0.00-0.15	10YR 3/2	g; wk; f	sandy	41.5
Sediment	0.16-0.37	10YR 4/3	sg	sandy	5.42
Ab	0.38-0.63	10YR 4/2	sb; wk; m	sandy	10.5
Eb	0.64-0.95	10YR 6/4	sg	sandy	4.0
Btb	>0.96	5YR 8/1	sb; md; m	sandy loam	6.9
		Pit 2 – T2			
A	0.00-0.09	5YR 4/1	g+sb; wk; f	sandy	22.4
Sediment 1	0.10-0.30	10YR 5/3	sg	sandy	5.4
Sediment 2	0.31-0.41	10YR 5/4	sg	sandy	5.8
Ab	0.41-0.65	5YR 4/1	sb; wk; m	sandy	7.6
Eb	0.65-1.10	10YR 5/4	sg	sandy	4.3
Btb	>1.10	5YR 8/1	sb; md; m	sandy loam	4.0
		Profile 1 – P1			
A	0.00-0.25	10YR 4/2	g+sb; wk; f	sandy	53.4
Sediment	0.26-0.40	10YR 5/4	sg	sandy	6.5
Ab	0.41-0.65	7.5YR 4/2	sb; wk; m	sandy	7.2
Eb	0.66-1.23	10YR 6/4	sb; md; m	sandy	4.0
Btb	>1.23	5YR 8/1	sb; md; m	sandy clay loam	4.3
		Profile 2 – P2			
A	0.00-0.20	5YR 4/1	g+sb; wk; f	sandy	19.5
Sediment 1	0.21-0.30	2.5Y 4/4	sg	sandy	6.5
Sediment 2	0.31-0.35	10YR 5/6	sg+sb; wk; m	sandy loam	4.7
Sediment 3	0.36-0.45	2,5Y 5/4	sg+sb; wk; m	sandy loam	7.2
Ab	0.46-0.65	10YR 3/3	sb; wk; m	sandy	12.2
Eb	0.66-1.23	10YR 5/4	sg	sandy	5.8
Btb	>1.23	5YR 8/1	sb; md; m	sandy loam	3.6

[(1)] Type: g - granular; sg - simple grain; ab - angular block; sb - subangular block. Grade: wk - weak; md - moderate, str - strong. Size: f - fine; m - medium; c - coarse.

In P1, the following sequence of soil horizons and sediment layers was found: A, sediment, Ab, Eb, and Btb (Figure 2c). The A horizon had a thickness of 0.25 m, a sandy texture, and a weak and fine granular and subangular blocky structure. This horizon had the highest OM content (53.4 g kg^{-1}) among the horizons and sediment layers studied. Only one type of sediment was found, which had a sandy texture and color and structure (simple grain) that differed from the under- and overlying horizons. The Ab horizon showed a slight increase in OM content in relation to the sediment layer, with low color values and chroma (Table 1). The Btb horizon had a structure with moderate, medium, subangular blocks and sandy clay loam texture.

In P2, the following sequence of soil horizons and sediment layers was found: A, sediment 1, sediment 2, sediment 3, Ab, Eb, and Btb (Figure 2d). The A horizon had a sandy texture, color 5YR 4/1, and granular and subangular blocky structure. Three types of sediment were identified by differences in thickness, color, texture, and structure. Unlike the other sediment layers in this study, the sediment 2 layer in this profile had a sandy loam texture and the lowest OM content (Table 1). The Ab horizon showed an increase in OM content compared to the sediment layers deposited above it, which conferred a darker color to this horizon. The Btb horizon had a moderate, medium, subangular blocky structure and a sandy loam texture.

In general, the sediments exhibited changes in color and structure compared to the underlying horizons (the Ab horizon) and the overlying A horizon. The A and Ab horizons, in all cases, exhibited darker colors (melanization), with low chroma, in comparison to

Figure 2. Images of the studied pits: soil horizons and sediment layers. (a) Pit 1 - T1; (b) Pit 2 - T2; (c) Profile 1 - P1; and (d) Profile 2 - P2.

the sediments, due to the increase in OM content. The morphological properties and increase in OM content in the Ab horizon helped identify this horizon as a paleo-horizon that was buried by the deposition of sediments on the surface. This buried horizon was used as important evidence in detecting *in situ* sedimentation zones (Turnage et al., 1997).

In addition to this, the development of a new A horizon with a weak structure in the first centimeters of the sediment layer occurred due to the accumulation of organic matter on the surface after deposition (Breemen and Buurman, 2002). This new A horizon manifested recent pedogenic processes (Buol et al., 2011), which would have occurred after implementation of the pine and guarantã reforestation. The presence of a new A horizon formed on the surface of the sediments confirms that there were no new deposits in these areas after reforestation and indicates that large scale erosion and, consequently, sedimentation processes no longer occur in these locations.

Reinforcing the idea that the sedimentation process occurred before or during the implementation of reforestation, the observations made in the vicinity of the pits and auger holes between TP1 and TP4 showed that the root collar of the trees that grow

in the study area were at ground level and were not covered or exposed by erosion processes (Figure 3). This observation is important because it shows that there was neither stem nor root collar burial due to erosive processes after reforestation, even though sediments with thicknesses of 0.30 m were concentrated at the drainage line currently occupied by the gully. It is also noteworthy that the gully located in the study area was opened after the sedimentation period, since the layers of sediment and the Ab horizon are exposed on the gully walls.

Reforestation formed a dense vegetation cover that favors soil and water conservation and reduces the erosion and sedimentation rates (Ouyang et al., 2013; Cândido et al., 2015). Such evidence suggest that the process of sediment deposition occurred during the period when this area was used for agriculture or in the transition period between agricultural usage and reforestation.

Distribution and geometry of the soil horizons and sediment layers

From the exploratory auger holes, five preferred deposition zones could be identified in the study area. These deposition zones occurred in well-defined locations along the drainage line of the area now occupied by a gully (Figure 4). The deposition zones have widths ranging from 5 to 7 m and lengths from 5 to 30 m. The deposition zones are bevel shaped, with the thickest side exposed on the wall of the gully. The maximum thickness varied according to the different deposition zones; zone 1 and 2 had a maximum thickness of 0.21 m, zone 3 of 0.14 m, and zone 4 of 0.30 m.

From detailed evaluation of the sediment deposition sites, it was possible to understand the distribution of the soil horizons and sediment layers, as well as the dominant deposition zones and their horizontal and vertical boundaries (Figure 5).

The TP1 segment (Figure 5a), characterized by successive auger holes, includes T1 and shows that the deposition area is located at the edges of the gully. The TP2 segment (Figure 5b) includes areas above and below T2 and shows two sediment deposition zones: one near the edge of the gully and the other half-way up the slope. The TP3 and TP4 segments are located upstream of P1 (Figure 5c) and P2 (Figure 5d), respectively, and both show deposition zones located at the edge of the gully.

Particle size analysis, flocculation, and statistical analysis of the sand fraction

Particle size distribution analysis of soils and sediments using a dispersant revealed an essentially sandy texture in the soil surface and a loamy sand texture in the subsurface for all pits and profiles analyzed. In the surface horizons, the clay content

Figure 3. Root collar of the trees that grow in the study area not covered nor exposed by erosion processes.

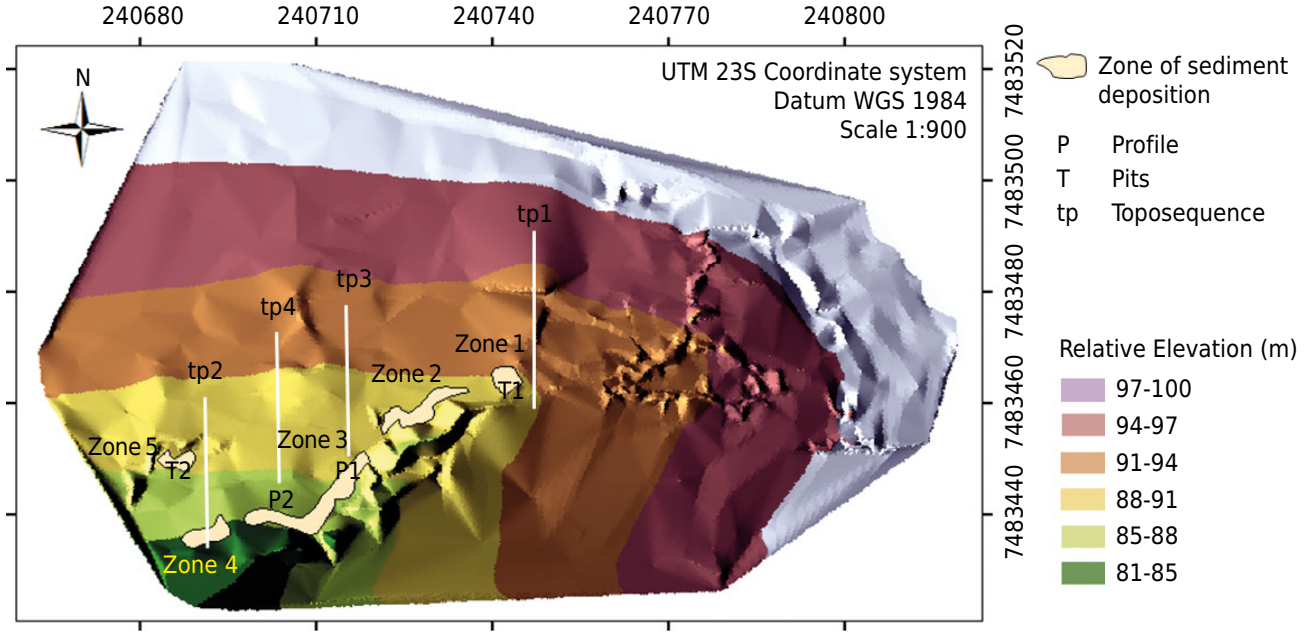

Figure 4. Digital model of the terrain showing the location of the sediment deposits.

did not exceed 100 g kg^{-1}, while in the subsurface horizons there was an increase in clay, ranging from 150 to 200 g kg^{-1} (Table 2).

With regard to the sediment layers, only sediment 2 from P2 had higher clay content (189 g kg^{-1}), qualifying for the loamy texture class. The remaining sediments are sandy, with an average of 58 g kg^{-1} of clay.

The results analyzed from samples dispersed in water from all pits and profiles showed a decrease in clay content levels and an increase in the silt fraction compared to the samples with total dispersion. This increase is more apparent in the Btb horizons and sediments 2 and 3 from P2, where the clay dispersed in water was zero, indicating that the clay in these layers remains aggregated in the presence of water in the form of silt or sand size aggregates, even after physical dispersion.

The increase in the silt fraction, with the exception of sediments 2 and 3 from P2, the decrease in the clay fraction, and the almost imperceptible change in the sand fraction all indicate that after a rain event, a portion of the clay particles in the sediments may have been transported in the form of silt size aggregates and not in dispersed form (Momoli et al., 2007; Oliveira et al., 2010). In the case of sediments 2 and 3 from P2, the clay fraction was transported entirely in the form of silt or fine sand size aggregates.

Clay aggregates, either sand or silt size, offer greater resistance to transport than fine primary dispersed particles, and respond in a way similar to silt and sand grains (Meyer et al., 1980), and are thus deposited together with these particles. This result has also been observed in other areas, where the clay particles transported in the form of aggregates resulted in changes in the transport dynamics by water (Sveistrup et al., 2008). These aggregates exhibited fine silt size (2-6 µm) or slightly larger.

The degree of flocculation was medium and low for the A and Ab horizons (Table 2). The lowest values were found in the Eb horizon for all pits and profiles, while higher degrees of flocculation were found in the Btb horizon, indicating a greater aggregation of colloidal particles in this horizon. Sediments showed medium to low degrees of flocculation, related to their simple grain structure, with the exception of sediments 2

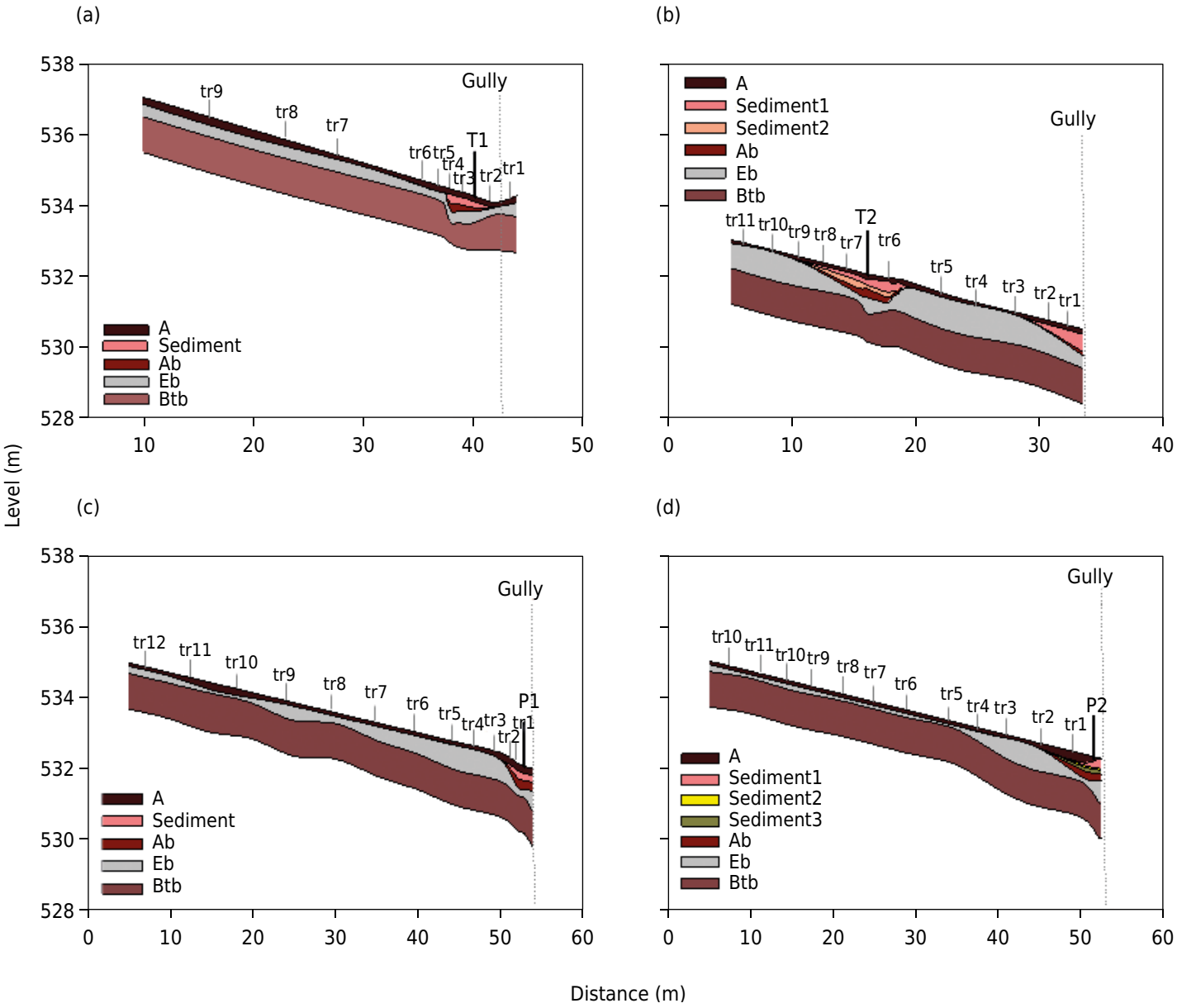

Figure 5. Structural analysis and two-dimensional distribution of TP1 segments (a), TP2 (b), TP3 (c), and TP4 (d).

and 3 of P2, which showed a degree of flocculation of 100 %, due to the low dispersion of clay in water. This low dispersion favored transport of these particles in the form of microaggregates of silt or fine sand sizes (Momoli et al., 2007), as explained above.

The sediments consisted mainly of sand, with the exception of sediment 2 from P2, which had a sandy loam texture. Statistical analysis of the sands showed similar results for all soil horizons and sediment layers, and revealed that fine sand was the predominant fraction both in the soil horizons and in the sediment layers. This dominance of fine sand is probably inherited from the local parent material, the Itararé Sandstone Formation, which has predominantly fine sand in its composition, among other fractions (Almeida et al., 1981; Arab et al., 2009). This similarity probably rules out the possibility that the deposited material originates from a lithologically different material (Schaetzl and Anderson, 2005; Schaetzl and Luehmann, 2013).

Practically all of the sediments were well sorted, except for the A horizons of the pits and sediment 1 from P1 and sediment 1 from T2, whose sand fraction was classified as moderately sorted (Table 2). In the sediments classified as well sorted, the skewness was approximately symmetrical, i.e., the mean diameter and the median were the same,

Table 2. Distribution of soil particles, degree of flocculation, and statistical parameters of the sand fraction in the soil horizons and sediment layers described in the pits and profiles

Horizon	Layer	With dispersant			Without dispersant			GF	Statistical parameters of the sand fraction	
		Clay	Silt	Sand	Clay	Silt	Sand		PSF (Medium)	Asymmetry
	m	g kg^{-1}						%		
					Pit 1 – T1					
A	0.00-0.15	36.5	248.9	714.6	11.9	206.1	782.0	67.4	FS	VNS
Sediment	0.16-0.37	53.6	155.1	791.4	34.5	191.8	773.6	35.6	FS	AS
Ab	0.38-0.63	59.8	192.6	747.5	48.2	196.5	755.3	19.4	FS	VNS
Eb	0.64-0.95	71.4	188.0	740.6	23.7	213.8	762.6	66.8	FS	VNS
Btb	>0.96	163.8	179.3	657.0	11.7	335.7	652.6	92.8	FS	VNS
					Pit 2 – T2					
A	0.00-0.09	49.4	120.6	830.0	24.2	138.9	836.9	51.1	FS	VNS
Sediment 1	0.10-0.30	57.6	124.4	818.0	48.1	130.0	821.9	16.4	FS	VNS
Sediment 2	0.31-0.41	46.6	125.4	828.0	35.9	149.0	815.2	23.0	FS	AS
Ab	0.41-0.65	60.2	170.9	768.9	36.8	205.2	758.0	39.0	FS	VNS
Eb	0.65-1.10	32.9	189.6	777.6	22.2	195.2	782.6	32.6	FS	AS
Btb	>1.10	199.0	190.5	610.5	11.8	376.5	611.6	94.0	FS	VNS
					Profile 1 – P1					
A	0.00-0.25	57.5	169.4	773.1	46.7	162.6	790.7	18.8	FS	VNS
Sediment	0.26-0.40	92.4	143.3	764.3	36.5	179.6	783.9	60.5	FS	VNS
Ab	0.41-0.65	59.8	145.6	794.6	34.7	170.6	794.7	41.9	FS	VNS
Eb	0.66-1.23	79.1	147.1	773.8	59.5	154.5	786.0	24.7	FS	VNS
Btb	>1.23	211.3	114.4	674.3	12.4	313.3	674.3	94.1	FS	VNS
					Profile 2 – P2					
A	0.00-0.20	59.2	168.0	772.8	36.2	173.7	790.1	38.8	FS	VNS
Sediment 1	0.21-0.30	71.6	185.6	742.9	60.2	226.6	713.2	15.9	FS	AS
Sediment 2	0.31-0.35	189.3	182.3	628.4	0.0	351.5	648.5	100.0	FS	AS
Sediment 3	0.36-0.45	144.1	203.8	652.1	0.0	324.0	676.0	100.0	FS	AS
Ab	0.46-0.65	81.9	164.7	753.4	54.9	195.2	749.9	32.9	FS	VNS
Eb	0.66-1.23	58.1	164.6	777.3	36.3	191.9	771.8	37.5	FS	VNS
Btb	>1.23	144.2	111.4	744.5	11.9	240.8	747.3	91.8	FS	VNS

PSF: predominant sand fraction (PSF); FS: fine sand; VNS: very negative skewed; AS: approximately symmetrical.

which demonstrates the high selection capacity of the erosive agent and, probably, the low transportation energy level of laminar flows (Suguio, 1973; Leeder, 1982).

In the other sediment layers classified as moderately sorted, the skewness was very negative, i.e., the average is less than the median; in this case, the distribution is skewed toward larger sand fractions (Suguio, 1973). These properties reflect a lower selection capacity and flows with greater energy in the transportation agents, tending to turbulent (Leeder, 1982; Ponçano, 1986). It should be noted that all the sediment layers that occupy a position in the pits and profiles closer to the surface showed a moderate degree of sorting and very negative skewness, whereas the deeper sediments were well sorted and approximately symmetrical. These properties of the sediments and their position in the pits, profiles, and landscape may feature two different deposition events in the study area. A first event (oldest), with the well-sorted material originating from low energy laminar transport processes, and a second later event with coarser material deposition, whose transport process showed a tendency of increased turbulence.

Soil micromorphology

For ease of understanding, micromorphological descriptions will be presented in groups based on the division of the soil horizons and sediment layers in the different profiles and pits. The dominant micromorphological properties of the soil horizons and sediment

layers will be described in the following order: A horizons, sediment layers, Ab horizons, Eb horizons, and Btb horizons.

The A horizons in the profiles and the pits had a gefuric-enaulic relative distribution with a $C/F_{2\mu m}$ ratio of 3:1 and a granular microstructure with a moderately to strongly developed pedality (Figure 6a). The fine material has dark coloration. In these horizons, compound impregnative nodules, typic nodules, amorphous nodules, and, more prominently, pores with loose continuous infillings are observed. Compound packing voids (80 %) dominate these horizons as a consequence of the granular microstructure, and vughs and channels (20 %) are also found. Moreover, decomposing roots, coprolites, and charcoal fragments were described. The coarse material exhibited a moderate degree of sorting, with subangular and angular grains with smooth surfaces.

Sediments in all profiles and pits were apedal, corroborating the simple grain structure with a mainly sandy texture found in the field. The coarse material was moderately to well-sorted. This material consisted of subangular and angular quartz grains with smooth surfaces. There were differences in the $C/F_{2\mu m}$ ratio between the sediment layers. For sediments in T1, T2, P1, and sediment 1 from P2, the $C/F_{2\mu m}$ ratio was 7:1, and in sediment layers 2 and 3 from T2, the $C/F_{2\mu m}$ ratio was 4:1.

The relative distribution of the sediments was chitonic in T1 and gefuric-chitonic in T2. P1 and P2 sediments had a simple grain and pellicular grain microstructure (Figure 6b). It is also noteworthy that in the sediment layers, a few isolated rounded microaggregates with a dark red color and sizes similar to the coarse silt and fine sand fractions were observed (Figure 6c).

The dominant porosity in the sediments was simple packing, with the presence of a few well-rounded vughs in all pits and profiles. T1 showed a higher number of simple packing voids (90 %) and a smaller number of rounded vughs (10 %) than T2, P1, and P2, which showed 70 % simple packing voids and 30 % rounded vughs. In these layers, which occupied <5 % of the thin section, various types of nodules were described, some with clay coating with a strong and continuous orientation and some with iron segregation features and dense incomplete infillings. In the sediments with a loamy sand texture (sediments 2 and

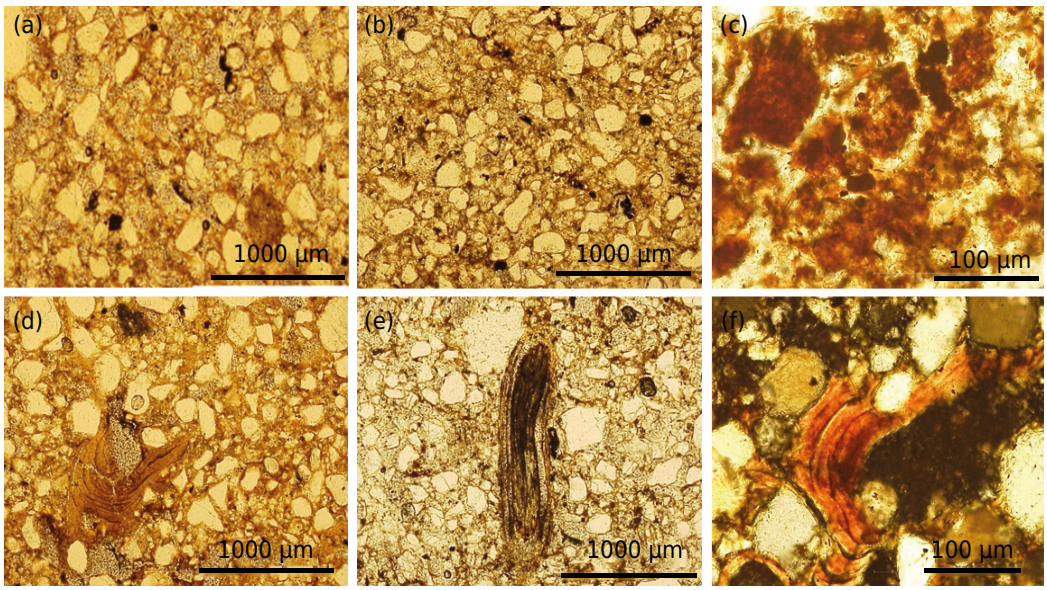

Figure 6. Microphotograph of sediment layers, A horizons and B horizons: (a) gefuric-enaulic relative distribution and granular microaggregates of moderately to strongly developed pedality in A horizons; (b) gefuric-chitonic relative distribution found in the sediments; (c) granular microaggregates found in sediments; (d) occurrence of fine material in loamy sand sediments; (e) biological activity: decomposing roots found in the Ab horizon; (f) dense and massive microstructure of the Btb horizons and dense incomplete clay infilling.

3 from P2), a greater quantity of fine material with a reddish color, together with iron and clay coatings, was observed (Figure 6d). Most of the fine material in these layers (sediments 2 and 3 from P2) was organized as microaggregates with coarse silt and fine sand sizes.

The Ab horizons had lower porosity than the A horizons and sediment layers. The porosity consisted of compound packing voids (90 %), channels, and vughs. The relative distribution is chitonic-gerufic, similar to the A horizons, but differs from the sediment layers (chitonic and gefuric-chitonic). They feature fine material with darkened coloration, corroborating the field descriptions and indicating organic material. Decomposing roots and charcoal fragments were described in these horizons (Figure 6e). The coarse fraction had a moderate degree of sorting and sub-angular and angular grains with smooth surfaces. The $C/F_{2\mu m}$ ratio was 4.5:1.

The Eb horizons had a chitonic-gefuric relative distribution with some monic zones and a pellicular grain microstructure (Figure 7a). These types of relative distributions and microstructures are essentially a consequence of the sandy texture property of these horizons (Table 1). Though less numerous than in other horizons, a few clay microaggregates were found. The dominant porosity was again the simple packing type. In this horizon, there was a smaller number of nodules than in the horizons above. The coarse fraction had a moderate degree of sorting, with subangular and angular grains with smooth surfaces. The $C/F_{2\mu m}$ ratio was 6:1.

The Btb horizons showed a higher amount of fine material (clay) than the other soil horizons and sediment layers, resulting in a porphyric relative distribution (Figure 7b) and a massive and dense microstructure (Figure 6f). Strongly and continuously oriented clay coatings and dense complete and dense incomplete infillings were observed (Figure 6f). The dominant porosity was classified as planar voids (60 %), with the presence of channels (20 %) and vughs (20 %). The coarse fraction had a moderate to poor degree of sorting composed of subangular and angular quartz grains with smooth surfaces. The $C/F_{2\mu m}$ ratio was 2:1.

Micromorphological descriptions of the soil horizons and sediment layers for the pits and profiles revealed differences in the $C/F_{2\mu m}$ ratio, relative distribution, microstructure, and the type of dominant voids. Differences observed in the soil organization helped clarify the sedimentation process and the organization of the sediment layers. The presence of a granular microstructure with moderate pedality and strong dark coloring in the A horizons in the pits and profiles studied showed the action of organic matter on the structuring of this horizon that originated from the deposited sediments. This micromorphological evidence reinforces the results obtained from the morphological descriptions in the field concerning formation of the A horizon on the surface of the deposited sediments after implementation of the reforestation project.

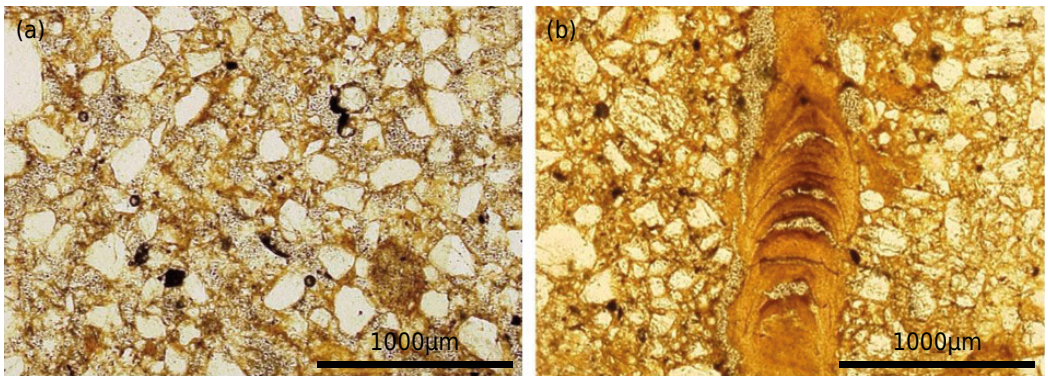

Figure 7. (a) Microphotograph of Eb horizons: chitonic-gefuric relative distribution with monic zones; pellicular grain microstructure. (b) Microphotograph Btb horizons: porphyric relative distribution; and massive and dense microstructure. Pores infilled by illuvial clay.

The presence of moderately- to well-sorted coarse material in the sediments indicates that runoff was not high in energy since only selective, non-turbulent flows would be able to transport and deposit particles of similar sizes (Parsons et al., 1991; Shi et al., 2012). These results corroborate the statistical results of the sand fraction, which also indicated uniformity in the size of the sand grains. The subangular and angular rounding of the coarse fraction of the sediments and soils indicates that these sediments may have a local origin and that the transport process covered only a short distance, which did not allow for abrasion and rounding of this material (Folk, 1978; Madhavaraju et al., 2009).

The sorting of the coarse material in the A horizons formed from the sediments, as well as the underlying sediment layers, revealed an improvement in this property in depth. The coarse material of the A horizon was classified as moderately sorted, whereas the underlying sediment was moderately to well sorted. This trend of improvement in the degree of sorting between the A horizons and the underlying sediment layers confirms the results obtained in the statistical analysis of the sand fraction using Falk and Ward's parameters, which corroborate the hypothesis that there were two separate episodes of transport and deposition, with different properties.

The profile located in the lower part of the landscape (P2) showed a higher concentration of clay and fine material in the sandy loam sediments than the other profiles and pits. Micromorphological evidence showed that part of the fine material was probably transported and deposited in the form of microaggregates. Another part might have been transported in a particulate form and deposited in the voids, as evidenced by the presence of voids coated and infilled with strongly oriented clay (Bertran and Texier, 1999). The increased amount of fine material in this landscape position, further downstream and at some depth relative to the rest of the sediment layers, strengthens the hypothesis of selective transport and deposition with a low energy level.

The Btb horizons showed typical features of a textural B horizon, with increased fine material, massive and dense microstructure, and coatings and infillings of illuvial clay in the voids. These properties were observed in other studies conducted on this type of soil in the region of the study site (Vidal-Torrado and Lepsch 1999; Mafra et al., 2001).

CONCLUSIONS

Sediments deposited in the study area appear to be derived from transport processes that occurred over short distances along the hillside slopes and from material detached from the local soils. This transport and deposition process, preceded by erosive events, would have occurred prior to reforestation of the area when the soils were used for agricultural purposes.

The analysis of morphological data (macro and micro) and the particle size distribution demonstrated two transportation and deposition events: the first, more selective in character and low in energy, and the second, less selective and with more turbulent flows.

Implementation of the reforestation project improved control over the erosion process through increased soil cover and formation of an A horizon on the surface of the deposited sediments, increasing their stability.

ACKNOWLEDGMENTS

Our thanks to the São Paulo Research Foundation (FAPESP) and the National Council for Scientific and Technological Development (CNPq) for granting scholarships and the research productivity fellowship.

REFERENCES

Almeida FFM. Mapa geológico do estado de São Paulo. São Paulo: Instituto de Pesquisas Tecnológicas; 1981. Esc 1: 500.000.

Arab PB, Perinotto JAJ, Assine ML. Grupo Itararé (P - C da bacia do Paraná) nas regiões de Limeira e Piracicaba - SP: contribuição ao estudo das litofácies. Geociências. 2009;28:501-21.

Bertran P, Texier JP. Facies and microfacies of slope deposits. Catena. 1999;35:99-121. https://doi.org/10.1016/S0341-8162(98)00096-4

Borrelli P, Märker M, Panagos P, Schütt B. Modeling soil erosion and river sediment yield for an intermountain drainage basin of the Central Apennines, Italy. Catena. 2014;114:45-58. https://doi.org/10.1016/j.catena.2013.10.007

Boulet R, Chauvel A, Humbel FX, Lucas Y. Analyse structurale et cartographic en pédologie. 1 – prise en compte de l'organisation bidimensionelle de la couverture pédologique: les études de toposéquences et leurs principaux apports a la connaissance des sols. Cahiers - ORSTOM. Série Pédologie. 1982;19:309-21.

Breemen NV, Buurman P. Soil formation. 2nd ed. Dordrecht: Kluwer Academic; 2002.

Bullock P, Fedoroff N, Jonguerius A, Stoops G, Tursina T. Handbook of soil thin section description. Wolverhampton: Waine Research Publication; 1985.

Buol SW, Southard RJ, Graham RC, McDaniel PA. 2nd ed. Soil Genesis and Classification. Iowa: Wiley-Blackwell; 2011.

Cândido BM, Silva MLN, Curi N, Freitas DAF, Mincato RL, Ferreira MM. Métodos de indexação de indicadores na avaliação da qualidade do solo em relação à erosão hídrica. Rev Bras Cienc Solo. 2015;39:589-97. https://doi.org/10.1590/01000683rbcs20140363

Castro SS, Cooper M, Santos MC, Vidal-Torrado P. Micromorfologia do solo: bases e aplicações. Tópic Cienc Solo. 2003;3:p.107-64.

Claessen MEC, organizador. Manual de métodos de análise de solo. 2a ed. Rio de Janeiro: Centro Nacional de Pesquisa de Solos; 1997.

Folk RL. Angularity and silica coatings of Simpson desert sand grains, Northern Territory, Australia. J Sedim Petrol. 1978;48:611-24.

Folk RL, Ward WC. Brazos River bar: a study in the significance of grain size parameters. J Sedim Petrol. 1957;27:3-26.

Gee GW, Or D. Particle-size analysis. In: Dane JH, Topp GC, editors. Methods of soil analysis. Physical methods. Madison: Soil Science Society of America; 2002. Pt. 4. p.255-93.

Gilbert ER, Camargo MG, Sandrini-Neto L. Rysgran: grain size analysis, textural classifications and distribution of unconsolidated sediments. R package version 2.0 [computer program]. 2012.

Grossman RB, Reinsch TG. Bulk density and linear extensibility. In: Dane JH, Topp GC, editors. Methods of soil analysis. Physical methods. Madison: Soil Science Society of America; 2002. Pt. 4. p.201-28.

Harmon WC, Meyer LD, Alonso CV. A new method for evaluating particle size distribution and aggregated portion of eroded sediment. Trans ASAE. 1989;32:89-96. https://doi.org/10.13031/2013.30967

Leeder MR. Sedimentology: process and product. Londres: Unwin Hyman; 1982.

Lima JEFW, Silva EM. Seleção de modelos para o traçado de curvas granulométricas de sedimentos em suspensão em rios. Rev Bras Eng Agric Amb. 2007;11:101-7. https://doi.org/10.1590/S1415-43662007000100013

Madhavaraju J, Barragán JCG, Hussain SM, Mohan SP. Microtextures on quartz grains in the beach sediments of Puerto Peñasco and Bahia Kino, Gulf of California, Sonora, México. Rev Mexic Cienc Geol. 2009;26:367-79.

Mafra AL, Silva EF, Cooper M, Demattê JLI. Pedogênese de uma seqüência de solos desenvolvidos de arenito na região de Piracicaba (SP). Rev Bras Cienc Solo. 2001;25:355-69. https://doi.org/10.1590/S0100-06832001000200012

Martínez-Mena M, Rogel JA, Albaladejo J, Castillo VM. Influence of vegetal cover on sediment particle size distribution in natural rainfall conditions in a semiarid environment. Catena. 1999;38:175-90. https://doi.org/10.1016/S0341-8162(99)00073-9

Martínez-Mena M, Castilho V, Albaladejo J. Relations between interril erosion processes and sediment particle size distribution in a semiarid Mediterranean area of SE of Spain. Geomorphology. 2002;45:261-75. https://doi.org/10.1016/S0169-555X(01)00158-1

Meyer LD, Harmon WC, Mcdowell LL. Sediment sizes eroded from crop row side slopes. Trans ASAE. 1980;23:891-8. https://doi.org/10.13031/2013.34682

Momoli RS, Cooper M, Castilho SCP. Sediment morphology and distribution in a restored riparian forest. Sci Agric. 2007;64:486-94. https://doi.org/10.1590/S0103-90162007000500006

Morgan RPC. Soil erosion and conservation. 3rd ed. Oxford: Blackwell Publishing; 2005.

Murphy CP, Bullock P, Turner RH. The measurement and characterization of voids in soil thin sections by image analysis: Part I: Principles and techniques. Eur J Soil Sci. 1977;28:498-508. https://doi.org/10.1111/j.1365-2389.1977.tb02258.x

Murphy CP. Thin section preparation of soils and sediments. Berkhamsted: AB Academic Publishers; 1986.

Nunes MCM, Cassol EA. Produção de sedimentos pela erosão em entressulcos em três Latossolos do Rio Grande do Sul. Rev Bras Eng Agric Amb. 2011;15:541-7. https://doi.org/10.1590/S1415-43662011000600001

Oliveira CA, Kliemann HJ, Correchel V, Santos FCV. Avaliação da retenção de sedimentos pela vegetação ripária pela caracterização morfológica e físico-química do solo. Rev Bras Eng Agric Amb. 2010;14:1281-7. https://doi.org/10.1590/S1415-43662010001200005

Ouyang Y, Leininger TD, Moran M. Impacts of reforestation upon sediment load and water outflow in the Lower Yazoo River Watershed, Mississippi. Ecol Eng. 2013;63:394-406. https://doi.org/10.1016/j.ecoleng.2013.09.057

Parsons AJ, Abrahams AD, Luk SH. Size characteristics of sediment in interrill overland flow on a semiarid hillslope, Southern Arizona. Earth Surf Proc Land. 1991;16:143-52. https://doi.org/10.1002/esp.3290160205

Pimentel D, Harvey C, Resosudarmo P, Sinclair K, Kurz D, McNair M, Crist S, Shpritz L, Fitton L, Saffouri R, Blair R. Environmental and economic costs of soil erosion and conservation benefits. Science. 1995;267:1117-23.

Ponçano WL. Sobre a interpretação ambiental de parâmetros estatísticos granulométricos: exemplos de sedimentos quaternários da costa brasileira. Rev Bras Geocienc. 1986;16:157-70.

Pope IC, Odhiambo BK. Soil erosion and sediment fluxes analysis: a watershed study of the Ni Reservoir, Spotsylvania County, VA, USA. Environ Monit Assess. 2014;186:1719-33. https://doi.org/10.1007/s10661-013-3488-5

Santos DS, Sparovek G. Retenção de sedimentos removidos de área de lavoura pela mata ciliar, em Goiatuba (GO). Rev Bras Cienc Solo. 2011;35:1811-8. https://doi.org/10.1590/S0100-06832011000500035

Santos HG, Jacomine PKT, Anjos LHC, Oliveira VA, Oliveira JB, Coelho MR, Lumbreras JF, Cunha TJF. Sistema brasileiro de classificação de solos. 3a ed. Rio de Janeiro: Embrapa Solos; 2013a.

Santos RD, Lemos RC, Santos HG, Ker JC, Anjos LH, Shimizu SH. Manual de descrição e coleta de solo no campo. 6a ed rev ampl. Viçosa, MG: Sociedade Brasileira de Ciência do Solo; 2013b.

Schaetzl R, Anderson S. Soils: genesis and geomorphology. Cambridge, UK: Cambridge University Press; 2005.

Schaetzl RJ, Luehmann, MD. Coarse-textured basal zones in thin loess deposits: products of sediment mixing and/or paleoenvironmental change? Geoderma.2013;192:277-85. https://doi.org/10.1016/j.geoderma.2012.08.001

Sharma PP. Interrill erosion. In: Agassi M, editor. Soil erosion conservation and rehabilitation. New York: Marcel Dekker; 1996. p.125-52.

Shi ZH, Fang NF, Wu FZ, Wang L, Yue BJ, Wu Gl. Soil erosion processes and sediment sorting associated with transport mechanisms on steep slopes. J Hydrol. 2012;454-455:123-30. https://doi.org/10.1016/j.jhydrol.2012.06.004

Soil Survey Staff. Keys to soil taxonomy. 12th ed. Washington, DC: United States Department of Agriculture, Natural Resources Conservation Service; 2014.

Stoops G, Jongerius A. Proposal for a micromorphological classification of soil materials. I. A classification of the related distributions of fine and coarse particles. Geoderma. 1975;13:189-99. https://doi.org/10.1016/0016-7061(75)90017-8

Stoops G. Guidelines for analysis and description of soil and regolith thin sections. Madison, WI: Soil Science Society of America; 2003.

Suguio K. Introdução à sedimentologia. São Paulo: Edgard Blücher; 1973.

Sveistrup TE, Marcelino V, Braskerud BC. Aggregates explain the high clay retention of small constructed wetlands: a micromorphological study. Boreal Environ Res. 2008;13:275-84.

Świtoniak M. Use of soil profile truncation to estimate influence of accelerated erosion on soil cover transformation in young morainic landscapes, North-Eastern Poland. Catena. 2014;116:173-84. https://doi.org/10.1016/j.catena.2013.12.015

Telles TS, Dechen SCF, Souza LGA, Guimarães MF. Valuation and assessment of soil erosion costs. Sci Agric. 2013;70:209-16. https://doi.org/10.1590/S0103-90162013000300010

Turnage KM, Lee SY, Foss JE, Kim KH, Larsen IL. Comparison of soil erosion and deposition rates using radiocesium, RUSLE, and buried soils in dolines in East Tennessee. Environ Geol. 1997;29:1-10. https://doi.org/10.1007/s002540050097

van Lier QJ, Vidal-Torrado P. PHI: Programa de microcomputador para análise estatística da granulometria de sedimentos. Rev Bras Cienc Solo. 1992;16:277-81.

Vidal-Torrado P, Lepsch IF. Relação material de origem/solo e pedogênese em uma sequência de solos predominantemente argilosos e latossólicos sobre psamitos na depressão periférica Paulista. Rev Bras Cienc Solo. 1999;23:357-69. https://doi.org/10.1590/S0100-06831999000200019

Wang ZJ, Jiao JY, Su Y, Chen Y. The efficiency of large-scale afforestation with fish-scale pits for revegetation and soil erosion control in the steppe zone on the hill-gully Loess Plateau. Catena. 2014;115:159-67. https://doi.org/10.1016/j.catena.2013.11.012

Young RA, Onstad CA, Bosch DD, Anderson WP. Agricultural non-point source pollution model: a watershed analysis tool. Washington, DC: United States Department of Agriculture; 1987. p.35-77.